Surfactants from the gas phase may enhance aerosol cloud nucleation

N. Sareen,[1,†] A. N. Schwier,[1] T. L. Lathem,[2] A. Nenes, [2,3,*] and V. F. McNeill[1,*]

1. Department of Chemical Engineering, Columbia University, New York, NY 10027 2. School of Earth and Atmospheric Sciences, Georgia Institute of Technology, Atlanta, GA 30332 3. School of Chemical and Biomolecular Engineering, Georgia Institute of Technology, Atlanta, GA 30332 †: Present address: Department of Environmental Sciences, Rutgers University, New Brunswick, NJ 08901

Submitted to Proceedings of the National Academy of Sciences of the United States of America

Clouds, a key component of the climate system, form when water vapor condenses upon atmospheric particulates termed Cloud Condensation Nuclei (CCN). Variations in CCN concentrations can profoundly impact cloud properties, with important effects on local and global climate. Organic matter (OM) constitutes a significant fraction of tropospheric aerosol mass, and can influence CCN activity by depressing surface tension, contributing solute, and influencing droplet activation kinetics by forming a barrier to water uptake. We present direct evidence that two ubiquitous atmospheric trace gases, methylglyoxal and acetaldehyde, known to be surface-active, can enhance aerosol CCN activity upon uptake. This effect is demonstrated by exposing acidified ammonium sulfate particles to 250 ppb or 8 ppb of gas-phase methylglyoxal and/or acetaldehyde in an aerosol reaction chamber for up to 5 h. For the more atmospherically relevant experiments, i.e. the 8 ppb organic precursor concentrations, significant enhancements in CCN activity, up to 7.5% reduction in critical dry diameter for activation, are observed over a timescale of hours, without any detectable limitation in activation kinetics. This reduction in critical diameter enhances the apparent particle hygroscopicity up to 26%, which for ambient aerosol would lead to cloud droplet number concentration increases of 8-10% on average. The observed enhancements exceed what would be expected based on Köhler theory and bulk properties. Therefore, the effect may be attributed to the adsorption of methylglyoxal and acetaldehyde to the gas-aerosol interface, leading to surface tension depression of the aerosol. We conclude that gas-phase surfactants may enhance CCN activity in the atmosphere.

atmospheric chemistry | climate | clouds

Introduction

The reactive uptake of volatile organic compounds (VOCs) by wet aerosols is a potentially important source of OM (1-3). The α-dicarbonyl species glyoxal and methylglyoxal, along with acetaldehyde and other carbonyl-containing species, belong to this class; they are absorbed by wet aerosol particles (or cloud droplets) and undergo aqueous phase reactions to form low-volatility secondary organic aerosol (SOA) (2, 4-6). The impacts of these processes on aerosol CCN activity and cloud droplet formation are unknown at this time. Few studies have focused on the impact of SOA generated in the aqueous phase on aerosol CCN activity (7-9). It was recently shown that the formation of SOA via the condensation of low-volatility VOC oxidation products, which are generally less hygroscopic than deliquescent inorganic salts, can affect the CCN activity of the seed aerosol (10-15). SOA generated through aqueous-phase chemistry is likely to be highly oxygenated and surface-active, hence making it strongly CCN active (6, 16, 17). Some of the VOC precursors themselves, including methylglyoxal and acetaldehyde, are also surface-active (6, 16, 17).

We studied the changes in the CCN activity of acidified ammonium sulfate seed aerosols upon exposure to gas-phase methylglyoxal or acetaldehyde. Both these organics are surface-active molecules and they also form surface-active material in aerosol bulk (6, 16, 17). A continuous flow streamwise thermal gradient CCN chamber (CFSTGC) was used downstream of a 3.5 m^3 Teflon reaction chamber or an aerosol flow tube in order to determine the cloud-forming potential of these aerosols after various exposure times. The critical dry diameters observed for each experiment as a function of instrument supersaturation are compared to the pure, non-acidified $(NH_4)_2SO_4$ control in order to demonstrate the effect of the organics. A decrease in critical activation diameter at a given critical supersaturation indicates enhancement in CCN activity, and vice versa. We find that, on the timescale of hours, methylglyoxal and/or acetaldehyde exposure enhances CCN activation beyond what is expected from Köhler theory predictions based on bulk properties. We attribute this enhancement to the surface adsorption of these VOCs from the gas-phase to the aerosol interface. To our knowledge, this is the first direct experimental evidence that the uptake of relatively insoluble, volatile organic gases by atmospheric aerosol particles may lead to an enhancement in cloud droplet formation and points to an unaccounted-for mechanism for augmenting CCN activity. This study introduces the idea that volatile organics in the atmosphere may act as a reservoir of surfactants that can be taken up by aerosol particles and augment their CCN activity.

Results and Discussion

Figure 1 summarizes the results of the CCN activation experiments showing the change in critical activation diameters as compared to pure $(NH_4)_2SO_4$ for the various conditions tested. (Figure S1 in the Supporting Information contains the supersaturation vs. activation diameter plots for each individual condition). After 3 minutes of exposure to 250 ppb methylglyoxal in the flow tube experiments (particle concentration $1.5\pm0.3\times10^5$ cm^{-3}), there is a negligible change in aerosol CCN activity. However, when aerosols ($9.7\pm0.3\times10^5$ cm^{-3}) are exposed to methylglyoxal for longer periods in the chamber (3-5 h), their CCN activity is enhanced considerably. For the conditions considered, methylglyoxal reduces the critical activation diameters of the inorganic seed aerosol on average by 6.36±0.05% at the supersaturations studied (0.2% to 1.0%). Acetaldehyde is another VOC which has been shown to depress surface tension in bulk aqueous ammonium sulfate solutions (6). Chamber experiments similar to those carried out with methylglyoxal were conducted using 250 ppb of acetaldehyde at an exposure time of 5 h. Acetaldehyde enhances

Reserved for Publication Footnotes

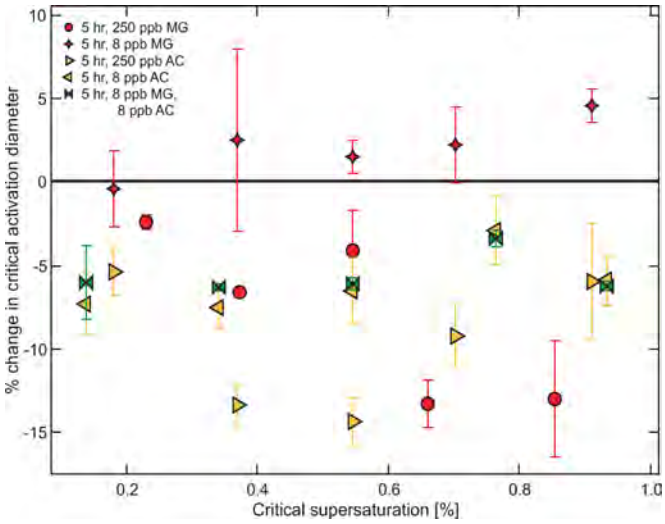

Fig. 1. : Cloud condensation nuclei (CCN) activity data. Humidified $(NH_4)_2SO_4$ aerosols were exposed to gas-phase methylglyoxal or acetaldehyde in a 3.5 m^3 Teflon reaction chamber. The critical dry diameters observed for each experiment as a function of instrument supersaturation are compared to the $(NH_4)_2SO_4$ control in order to demonstrate the effect of organics. A decrease in critical activation diameter at a given critical supersaturation indicates enhancement in CCN activity, and vice versa. The data shown here are the results for $(NH_4)_2SO_4$ particles exposed to 250 ppb and 8 ppb of methylglyoxal for 5 h, particles exposed to 250 ppb and 8 ppb of acetaldehyde for 5 h, and finally particles exposed to a mixture of 8 ppb of methylglyoxal and 8 ppb of acetaldehyde for 5 h.

Table 1.

Experiment	Average κ
$(NH_4)_2SO_4$	0.60±0.18
5 hr 250 ppb MG	0.81±0.24
3 hr 250 ppb MG	0.74±0.22
3 min 250 ppb MG	0.63±0.18
5 hr 8 ppb MG	0.55±0.16
3 min 8 ppb MG	0.59±0.18
5 hr 250 ppb AC	0.81±0.24
5 hr 8 ppb AC	0.72±0.22
5 hr 8 ppb AC, 8 ppb MG	0.71±0.19

CCN activity even more than methylglyoxal, reducing the critical activation diameters on average by 9.68±0.04%.

Methylglyoxal and acetaldehyde have been observed in both marine and continental environments (18-23). The gas-phase methylglyoxal, acetaldehyde, and particle concentrations used in the experiments described above exceed typical atmospheric concentrations (urban: 10^4 cm^{-3}, 2.5 ppb methylglyoxal, 4 ppb acetaldehyde (24, 25); wet-season Amazon: 10^2 cm^{-3}, 0.125 ppb methylglyoxal (18, 26), 0.5 ppb acetaldehyde (27)). Chamber experiments conducted at lower acetaldehyde and particle concentrations ($2.58x10^4$ cm^{-3}, 8 ppb acetaldehyde) with a 5 h residence time showed a depression in critical activation diameters by 6.01±0.02% at the supersaturations studied (Figure 1). However, experiments conducted at low methylglyoxal and particle concentrations ($1.78x10^4$ cm^{-3}, 8 ppb methylglyoxal) showed CCN activity approaching that of ammonium sulfate.

Table 1 lists the average apparent hygroscopicity parameter, κ (calculated from the CCN activity data following Petters and Kreidenweis (28) and following the convention that $\sigma=\sigma_{water}$) for each experiment. (Figure S2 in the Supporting Information shows the change in κ as compared to $(NH_4)_2SO_4$). For the 3 min methylglyoxal flow tube experiments, the κ values (0.63±0.18) are consistent with pure $(NH_4)_2SO_4$. Particles exposed for longer time scales, however, show an increase in κ (beyond that of pure $(NH_4)_2SO_4$) with increasing supersaturation. Exposure to 250 ppb methylglyoxal in the chamber increases the apparent hygroscopicity from ~0.6 to ~1.0. Particles exposed to 250 ppb acetaldehyde become substantially more hygroscopic than pure ammonium sulfate, with κ values ranging from 0.62 to 1.00 (the highest observed κ value for the 8 ppb exposure experiments was 0.88).

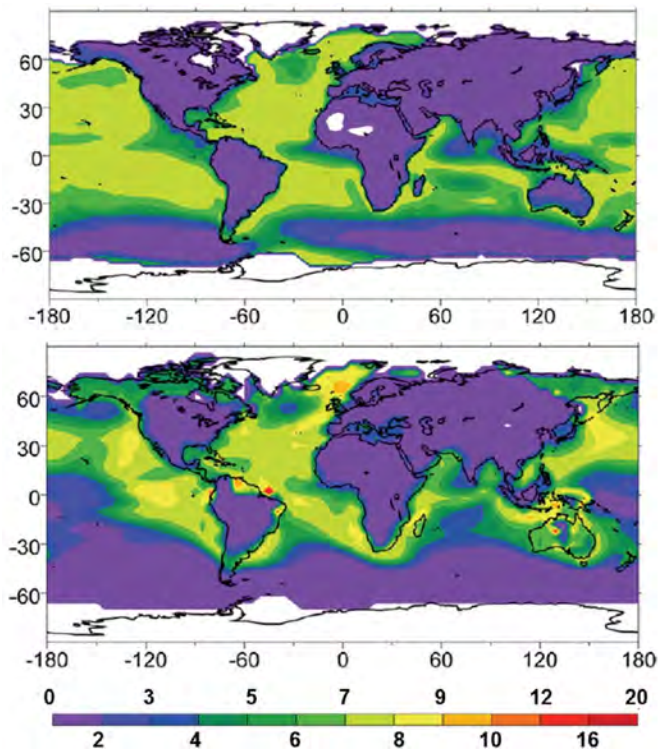

Fig. 2. : Stratus cloud CDNC response (%) to an aerosol κ increase of 20%. Results are shown for the GEOS-CHEM (top panel) and NASA-GMI (bottom panel) models coupled with the cloud droplet adjoint framework of Karydis et al. (2012) (29). For a 40% (60%) perturbation in κ, multiply legend by a factor of 2 (3). CDNC changes were calculated by multiplying the direct sensitivity of CDNC to kappa, ∂CDNC/∂κ (computed by the adjoint method) with the κ perturbation, as CDNC responds linearly to κ for this range of variation (not shown). For more information on the simulations, refer to (29).

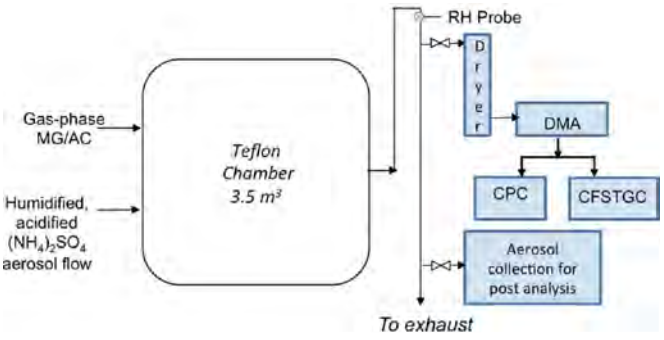

Fig. 3. : Schematic of the experimental setup. Gas phase methylglyoxal and/or acetaldehyde and ammonium sulfate seed aerosols are introduced into the chamber maintained at 62-67% RH. At the outlet, particles are analyzed using a SMPS and a CFSTGC.

Such shifts in hygroscopicity could lead to important enhancements in cloud droplet number concentrations (CDNC). Simulations using the GEOS-CHEM and NASA-GMI models coupled with the cloud droplet adjoint framework of Karydis et al. (29) were conducted in order to understand the stratus cloud CDNC response to a hypothetical 20% increase in hygroscopicity (reflecting what was observed in the 8ppb acetaldehyde exposure experiments). Figure 2 shows that these global models predict that CDNC increases on average by 10%, and by as much as 20% over continental regions. Given that marine stratocumulus clouds are strong climate forcers and are sensitive to CCN concentration changes, a 10% increase in CDNC would be important. To the extent that liquid water is not affected, such a CDNC perturbation could lead to roughly a 4% decrease in cloud droplet effective radius. This could change shortwave cloud albedo by up to 0.7% (30), which if globally relevant would exert a -0.5 W m^{-2} radiative cooling. Although not all stratus are expected to be affected and manifest this cooling, this simple calculation illustrates the potential impact of this phenomenon on calculations of shortwave cloud forcing.

Given that organics generally exhibit more than twofold *lower* κ than $(NH_4)_2SO_4$, (28) the aerosol surface tension must be lower than that of pure water to explain the increase in κ that we observe (31). κ was observed to increase at higher supersaturations. As another way of expressing this, the observed critical supersaturation in our experiments (S_c) deviates somewhat from the power law dependence on dry diameter (d_d) predicted by simple Köhler theory ($S_c \sim d_d^{-1.5}$); power law exponents range from -1.28 for the 5 h experiments to -1.51 for 3 min exposures (Supporting Information, Table S1). This is indicative of surfactants being present, as particles activating at higher supersaturations (i.e. smaller particles) tend to be more concentrated in surfactants at the critical wet diameter, resulting in a greater surface tension reduction than in particles which activate at lower supersaturations. This is applicable when surface-bulk partitioning of organics does not fully compensate for surface tension depression (32), and if surfactants are in equilibrium with the bulk and gas phase.

Köhler Theory Analysis (KTA) (33) was used to infer the extent of surface tension depression (with respect to water) in the particles. The relative abundance of the organic and inorganic components was obtained from water-soluble organic carbon (WSOC) analysis and ion chromatography (IC) of aqueous extracts of filter samples (by pumping down the chamber for approximately 14 h following an exposure experiment with 250 ppb of methylglyoxal and 5h residence time). KTA suggests that methylglyoxal and its reaction products suppress the surface tension of the aerosols to 65.1±0.8 dyn cm^{-1} compared to 72.55 dyn cm^{-1} for water. Methylglyoxal and acetaldehyde have low effective Henry's Law constants compared to that of glyoxal (34). In accord with the observations of Kroll et al. (2005) (3), we observed negligible particle growth when inorganic seed particles with a diameter of 150 nm were size-selected using a differential mobility analyzer (DMA, TSI) and exposed to methylglyoxal in the chamber (Supporting Information, Figure S3). This suggests that the surface-active organic species in this study reside at the gas-aerosol interface and induce the significant effects on CCN activity observed mainly by altering the properties of the particle surface. This is consistent with observation by Jayne et al. that acetaldehyde uptake by liquid water droplets on short timescales is pH-dependent and exceeds predictions based on bulk-phase parameters (35). This is the first time that the presence of relatively insoluble VOCs has been shown to enhance aerosol CCN activity.

If the total uptake of methylglyoxal to the particles is described by Henry's Law, then based on an effective Henry's Law constant of $H^* = 3.2 \times 10^4$ M atm^{-1} (34), and experimental surface tension data for aqueous bulk methylglyoxal solutions (16) (which is an upper limit in surface tension change given that bulk-surface repartitioning will mitigate some of the surfactant impacts on κ) the surface tension of the particles exposed to 250 ppb of methylglyoxal at the moment of activation is predicted to be 72.02 dyn cm^{-1}. This leads to a very small predicted change in κ (2.2% increase relative to pure ammonium sulfate). A similar calculation for acetaldehyde, which has a Henry's Law constant two orders of magnitude lower than that of methylglyoxal (34), predicts an insignificant change in κ (0.01% increase). If surface-bulk repartitioning of the solute had been dominant, it would have depressed hygroscopicity further when compared to the pure inorganic. Romakkaniemi et al. (2011) modeled a similar system, specifically the reactive uptake of gas-phase methylglyoxal to $(NH_4)_2SO_4$ aerosol, allowing aqueous-phase OH oxidation to take place (36). They predicted that total reactive uptake of surface-active species into the aqueous phase may be enhanced by surface-bulk partitioning, especially for small particles, beyond what would be predicted based on Henry's Law alone. The significant differences between the model system of Romakkaniemi et al. and our study are that 1) the additional driving force for uptake of the aerosol-phase OH reaction with the organics is absent in our experiments and 2) they assume equilibrium between the gas, surface, and bulk. The fact that we observe a much greater enhancement in κ than predicted solely based on Henry's Law, and that no chemical change in the bulk or surface composition will induce a Raoult effect that increases κ beyond that of pure $(NH_4)_2SO_4$, suggests that surface adsorption plays a significant role in determining the aerosol surface tension and thus CCN activity (1, 37).

To confirm that changes in bulk hygroscopicity cannot explain the κ enhancements seen in the chamber data, we analyze the CCN activity of atomized aqueous filter extracts to quantify hygroscopicity of the bulk material in the aerosol. By comparing this hygroscopicity to that of the chamber aerosol, we can deduce changes related to surface processes and non-equilibrium phenomena occurring in the chamber. Aerosolized filter extracts show similar CCN activity to that of pure $(NH_4)_2SO_4$, but much less than that of particles exposed to methylglyoxal in the aerosol chamber for 3-5 h (Supporting Information, Figure S4). Similar results to the filter extracts were observed for aerosols formed by atomizing bulk aqueous solutions of 3.1 M $(NH_4)_2SO_4$ and 0.5 M methylglyoxal 24 h after mixing (previously shown to exhibit significant surface tension depression) (16). Aerosols formed from atomized solutions of 0.5 M methylglyoxal and/or 0.5 M acetaldehyde and Millipore water exhibit decreased CCN activity compared to pure $(NH_4)_2SO_4$, typical of pure organic aerosols ($\kappa = 0.12 \pm 0.04$) and drastically different from the observed chamber aerosol hygroscopicity (Supporting Information, Figure S5). This supports the notion that surface adsorption of methylglyoxal and acetaldehyde (not present in the atomized solution experiments) is key to the CCN enhancement seen in the particles sampled directly from the chamber, as the hygroscopicity of aerosol generated from bulk solutions never exceeds that of the pure salt.

Comparing our results for the flow tube and chamber exposure studies suggests that a timescale of 3 min $< \tau <$ 3 h is required for surface modification and the concomitant enhancement in CCN activity. This could suggest a slow approach to adsorption equilibrium, or that formation of oligomers in the near-surface region is required. Hydration of methylglyoxal in the aqueous phase occurs on a timescale of ~1 s (38). The timescale of methylglyoxal self-oligomerization reactions is on the order of hours (16) in saturated ammonium sulfate solutions (full details of the timescale analysis are given in the Supporting Information). Recent studies of acetaldehyde and methylglyoxal mixtures in bulk ammonium sulfate solutions showed that cross-reactions between the two organics lead to greater surface tension

depression than predicted based on the single-species isotherms (6). To represent a more atmospherically relevant environment, the combined effect of these aldehydes was also studied in the chamber; 2.33x10^4 cm^{-3} of acidified ammonium sulfate were exposed to 8 ppb each of methylglyoxal and acetaldehyde for 5 h. These experiments showed similar CCN enhancement to the low concentration acetaldehyde experiments. Unlike the bulk experiments of Li et al. (2011), no synergistic effect due to the mixed organics was observed. This suggests that the mechanism of surface tension depression is different in the bulk system vs. the aerosols, and that the formation of oligomer cross products may be more important to surface tension depression in the bulk system.

The possibility of phase separation when the particles enter the dryer/CFSTGC setup can be ruled out based on a number of factors: the aerosol was acidified, preventing complete drying, thereby, preserving the gas-liquid interface. Additionally, particle growth in the dry distribution was not observed hence the amount of organic material is small and this reduces the chances for a phase separation. The state behavior of the particles at higher and lower relative humidities is also predictable, suggesting that two-phase separation is unlikely (Supporting Information).

The wet diameter profiles of the activated droplets formed by the particles exposed to methylglyoxal and/or acetaldehyde at all time scales studied are similar to that of pure $(NH_4)_2SO_4$. These observations rule out the possibility of a kinetic barrier to water uptake to these particles on the timescale of the CCN measurements (39). However, the barrier action of a surfactant film towards the uptake of gas-phase species to the particle depends on the identity of the penetrating gas-phase molecules. Hence, a barrier effect for the uptake of trace gases (with implications for aerosol heterogeneous chemistry) is a question for future study.

Conclusions

We report here the results of chamber experiments conducted to study how the uptake of two VOCs in the atmosphere, methylglyoxal and acetaldehyde, on acidified $(NH_4)_2SO_4$ seed aerosols can affect their CCN activity. At 250 ppb, both organics individually enhanced CCN activity. At more atmospherically relevant concentrations of 8 ppb, acetaldehyde depressed the critical activation diameters, whereas no change was seen with methylglyoxal. A mixture of the two organics at lower concentrations showed comparable augmentation in CCN activity to 8 ppb acetaldehyde alone. These enhancements are beyond what are expected due to Henry's Law alone and can be attributed to surface adsorption and non-equilibrium partitioning between the gas and aerosol phases. Based on the maximum enhancements seen in our experiments, a similar surfactant effect occurring in the atmosphere may increase calculated average cloud droplet number concentrations by 8-10%, thus affecting predictions of shortwave cloud albedo. This is the first experimental study where such an effect has been demonstrated and it is likely that a similar effect may also be observed in ambient aerosols in the presence of a mixture of surface-active VOCs. It is interesting to note that droplet closure studies in polluted ambient clouds (e.g., Conant et al., 2003; Fountoukis et al., 2007; Meskhidze et al., 2005) (40-42) do not account for surfactant adsorption effects but require an assumption of water uptake coefficient, γ, that is considerably lower (γ = 0.03 - 0.06) than theoretical expectations or in-situ CCN activation experiments (γ = 0.2 – 1.0) (43-49). This discrepancy in uptake coefficient elevates CDNC in ambient clouds by up to 20% (41), consistent with the magnitude of the surfactant effects observed in our study. Therefore, although surfactant adsorption effects on droplet number have not been identified in ambient aerosol to date, the aforementioned discrepancy in water uptake coefficient may by a direct consequence of it. To demonstrate that the observed effects occur in the atmosphere, future field studies in regions with high VOC concentrations should be conducted by exposing $(NH_4)_2SO_4$ seed aerosols to ambient air in an aerosol chamber and using similar CCN and filter analyses to those done in our laboratory chamber experiments. Alternatively, particles under stable equilibrium with supersaturated water vapor can be suspended using an electrodynamic balance (50), and then exposed to the organic gas-phase precursors to examine whether nucleation is induced in accord with our measurements. Finally, exposing particles from the chamber experiments carried out here to ultra-high RH can deconvolute the contribution of bulk solute and surface tension depression to the observed hygroscopicity. (51) Future work using these methods will help determine whether these mechanisms occur in the atmosphere.

Methods

A schematic of the experimental setup is shown in Figure 3. A 0.2 M $(NH_4)_2SO_4$ solution was prepared using Millipore water and the pH was adjusted to 0±0.1 or 2±0.1 using H_2SO_4, as the reactions which drive uptake are thought to be promoted by an acidic environment (16). The solution was aerosolized with pure N_2 using a constant output atomizer (TSI). This wet aerosol stream was exposed to either gas-phase methylglyoxal (250 ppb or 8 ppb) and/or acetaldehyde (250 ppb or 8 ppb) in a continuous-flow 3.5 m^3 Teflon aerosol chamber. The organic trace gas and acidified $(NH_4)_2SO_4$ particles were added into the chamber together at a total flow rate of 13 LPM for a typical residence time of ~5 h. As predicted based on a mass balance on the aerosol chamber (Supporting Information) and confirmed using Chemical Ionization Mass Spectrometry (CIMS) measurements of gas-phase methylglyoxal concentrations during a typical experiment, the gas-phase organic is not significantly depleted in our experiments. Hence, we do not need to take into account depletion when calculating potential effects as considered by Kulmala et al. (1993) and follow up studies (52). To characterize the time evolution of these processes, a residence time of 3 h was also tested using the chamber, and a glass flow tube (7.5 cm ID, 55 cm length) was used for a 3 min exposure time. Relative humidity inside the reactors was maintained between 62-67% as measured with a relative humidity meter (Vaisala) by passing the N_2 dilution flow though a bubbler filled with Millipore water. At the outlet of each reactor, the particles were passed through a diffusion dryer, a scanning mobility particle sizer (SMPS, TSI) and a CFSTGC (Droplet Measurement Technologies) to monitor particle concentration and CCN activity, respectively, using Scanning Mobility CCN Analysis (SMCA) (53). Total aerosol number concentrations in the chamber were 9.7±0.3×10^5 cm^{-3} (in the aerosol flow tube experiments, 1.5±0.3×10^5 cm^{-3}). The size distribution had a mean volume-weighted particle radius of 231±1.3 nm with a geometric standard deviation of 1.4 (mean surface-weighted particle radius was 203±1.7 nm with a geometric standard deviation of 1.6).

The pure $(NH_4)_2SO_4$ (non-acidified) solution was aerosolized, passed through a diffusion drier, and analyzed using SMCA to obtain the salt control. A control experiment with only the inorganic seed aerosol being introduced into the chamber was also conducted and analyzed, and the results were consistent with the pure $(NH_4)_2SO_4$ solution data. Bulk aqueous solutions containing 0.5 M of the organic (methylglyoxal and/or acetaldehyde) in solution form with and without 3.1 M $(NH_4)_2SO_4$ were allowed to react for 24 h, and were then atomized and analyzed in a similar manner. For select experiments, the $(NH_4)_2SO_4$/methylglyoxal particles were passed through a heated stainless steel tube at 100°C upstream of the SMPS/CFSTGC. No appreciable difference in the CCN activity spectra was observed with and without heating, suggesting that CCN activity in this system is not affected by volatilization biases (54).

At the end of each chamber experiment, particles from the chamber were collected on Zeflour filters (Pall, 47 mm, 2.0 µm) for ~ 14 h at a pumping rate of 14 LPM, where 7 LPM was the chamber effluent and the rest of the flow consisted of dry N_2 in order to avoid deliquescence of the filter-sample aerosol. The water-soluble fraction of the collected particles was analyzed following the procedures of Asa-Awuku et al. (2010) (33): the filters were extracted in 8 mL of pure water (18 MΩ) during a 1.25 h sonication process in a water bath heated to approximately 60°C. The filter extracts were then analyzed for WSOC concentration with a Total Organic Carbon (TOC) Turbo Siever analyzer, for soluble anion and cation composition with an Ion Chomatography system (Dionex DX-500); the CCN activity of the samples was measured by atomizing 3-5 mL of the extracted sample in a collision-type atomizer, drying the aerosol stream with two diffusion dryers, and analyzing using SMCA as described for the chamber experiments. The hygroscopicity of each filter extract was then determined with respect to a pure water blank. Gas-phase methylglyoxal was prepared as described previously by Kroll et al. (2005) (3), except that it was collected in a cold finger at -70 °C. While at this temperature, a 5 sccm or 0.5 sccm N_2 stream was passed though the cold finger for a final concentration of 250 ppb or 8 ppb in the aerosol reaction chamber. Acetaldehyde was prepared by adding 99.9 wt% liquid acetaldehyde (Sigma Aldrich) to a cold finger under an oxygen-free

environment and then passing a 1.4 sccm N_2 stream over it while the cold finger was kept at -78 °C for a final concentration of 250 ppb or passing a 0.3 sccm N_2 stream over it while the cold finger was kept at -92 °C for a final concentration of 8 ppb.

Acknowledgements.

This work was funded by the NASA Tropospheric Chemistry program (grant NNX09AF26G) and the ACS Petroleum Research Fund (grant 48788-DN14). AN acknowledges support from an NSF CAREER award. TLL acknowledges support from a NSF Graduate Research Fellowship and a Georgia Tech Institutional Fellowship. We are grateful to Prof. Rodney Weber for use of the filter sampling apparatus, Total Organic Carbon Turbo Siever analyzer, and helpful discussions. We also thank Prof. Armistead Russell and Marcus Trail for use of their Dionex DX-500 Ion Chromatograph.

1. Donaldson DJ & Vaida V (2006) The influence of organic films at the air-aqueous boundary on atmospheric processes. *Chem. Rev.* 106(4):1445-1461.
2. Ervens B & Volkamer R (2010) Glyoxal processing by aerosol multiphase chemistry: towards a kinetic modeling framework of secondary organic aerosol formation in aqueous particles. *Atmos. Chem. Phys.* 10(17):8219-8244.
3. Kroll JH, *et al.* (2005) Chamber studies of secondary organic aerosol growth by reactive uptake of simple carbonyl compounds. *J. Geophys. Res.* 110(D23):D23207.
4. Nozière B, Dziedzic P, & Cordova A (2010) Inorganic ammonium salts and carbonate salts are efficient catalysts for aldol condensation in atmospheric aerosols. *Phys. Chem. Chem. Phys.* 12(15):3864-3872.
5. Tan Y, Carlton AG, Seitzinger SP, & Turpin BJ (2010) SOA from methylglyoxal in clouds and wet aerosols: Measurement and prediction of key products. *Atmos. Environ.* 44(39):5218-5226.
6. Li Z, Schwier AN, Sareen N, & McNeill VF (2011) Reactive processing of formaldehyde and acetaldehyde in aqueous aerosol mimics: Surface tension depression and secondary organic products. *Atmos. Chem. Phys.* 11(22):11617-11629.
7. Bilde M & Svenningsson B (2004) CCN activation of slightly soluble organics: the importance of small amounts of inorganic salt and particle phase. *Tellus B* 56(2):128-134.
8. Cruz CN & Pandis SN (2000) Deliquescence and hygroscopic growth of mixed inorganic-organic atmospheric aerosol. *Environ. Sci. Technol.* 34(20):4313-4319.
9. Prenni AJ, *et al.* (2001) The effects of low molecular weight dicarboxylic acids on cloud formation. *J. Phys. Chem. A* 105(50):11240-11248.
10. Duplissy J, *et al.* (2008) Cloud forming potential of secondary organic aerosol under near atmospheric conditions. *Geophys. Res. Lett.* 35(3):L03818.
11. Engelhart GJ, Asa-Awuku A, Nenes A, & Pandis SN (2008) CCN activity and droplet growth kinetics of fresh and aged monoterpene secondary organic aerosol. *Atmos. Chem. Phys.* 8 (14):3937-3949.
12. King SM, Rosenoern T, Shilling JE, Chen Q, & Martin ST (2009) Increased cloud activation potential of secondary organic aerosol for atmospheric mass loadings. *Atmos. Chem. Phys.* 9(9):2959-2971.
13. Prenni AJ, Petters MD, Kreidenweis SM, DeMott PJ, & Ziemann PJ (2007) Cloud droplet activation of secondary organic aerosol. *J. Geophys. Res.* 112(D10):D10223.
14. VanReken TM, Ng NL, Flagan RC, & Seinfeld JH (2005) Cloud condensation nucleus activation properties of biogenic secondary organic aerosol. *J. Geophys. Res.* 110(D7):D07206.
15. Engelhart GJ, Moore RH, Nenes A, & Pandis SN (2011) Cloud condensation nuclei activity of isoprene secondary organic aerosol. *J. Geophys. Res.* 116(D2):D02207.
16. Sareen N, Schwier AN, Shapiro EL, Mitroo D, & McNeill VF (2010) Secondary organic material formed by methylglyoxal in aqueous aerosol mimics. *Atmos. Chem. Phys.* 10 (3):997-1016.
17. Schwier AN, Sareen N, Mitroo D, Shapiro EL, & McNeill VF (2010) Glyoxal-methylglyoxal cross-reactions in secondary organic aerosol formation. *Environ. Sci. Technol.* 44(16):6174-6182.
18. Fu TM, *et al.* (2008) Global budgets of atmospheric glyoxal and methylglyoxal, and implications for formation of secondary organic aerosols. *J. Geophys. Res.* 113(D15):D15303.
19. Lewis AC, *et al.* (2005) Sources and sinks of acetone, methanol, and acetaldehyde in North Atlantic marine air. *Atmos. Chem. Phys.* 5(7):1963-1974.
20. Millet DB, *et al.* (2010) Global atmospheric budget of acetaldehyde: 3-D model analysis and constraints from in-situ and satellite observations. *Atmos. Chem. Phys.* 10(7):3405-3425.
21. Seaman VY, Charles MJ, & Cahill TM (2006) A sensitive method for the quantification of acrolein and other volatile carbonyls in ambient air. *Anal. Chem.* 78(7):2405-2412.
22. Zhou X & Mopper K (1990) Measurement of sub-parts-per-billion levels of carbonyl compounds in marine air by a simple cartridge trapping procedure followed by liquid chromatography. *Environ. Sci. Technol.* 24(10):1482-1485.
23. Zhou X & Mopper K (1990) Apparent partition coefficients of 15 carbonyl compounds between air and seawater and between air and freshwater; implications for air-sea exchange. *Environ. Sci. Technol.* 24(12):1864-1869.
24. Grosjean E, Grosjean D, Fraser MP, & Cass GR (1996) Air quality model evaluation data for organics. 2. C1 - C14 carbonyls in Los Angeles air. *Environ. Sci. Technol.* 30(9):2687-2703.
25. Hughes LS, Cass GR, Gone J, Ames M, & Olmez I (1998) Physical and chemical characterization of atmospheric ultrafine particles in the Los Angeles area. *Environ. Sci. Technol.* 32(9):1153-1161.
26. Roberts GC, Nenes A, Seinfeld JH, & Andreae MO (2003) Impact of biomass burning on cloud properties in the Amazon Basin. *J. Geophys. Res.* 108(D2):4062.
27. Kesselmeier J, *et al.* (2002) Concentrations and species composition of atmospheric volatile organic compounds (VOCs) as observed during the wet and dry season in RondÙnia (Amazonia). *J. Geophys. Res.* 107(D20):8053.
28. Petters MD & Kreidenweis SM (2007) A single parameter representation of hygroscopic growth and cloud condensation nucleus activity. *Atmos. Chem. Phys.* 7(8):1961-1971.
29. Karydis VA, Capps SL, Russell AG, & Nenes A (2012) Adjoint sensitivity of global cloud droplet number to aerosol and dynamical parameters. *Atmos. Chem. Phys.* 12(19):9041-9055.
30. Seinfeld JH & Pandis SN (2006) *Atmospheric Chemistry and Physics - From Air Pollution to Climate Change (2nd Edition)* (John Wiley & Sons).
31. Ruehl CR, Chuang PY, & Nenes A (2010) Aerosol hygroscopicity at high (99 to 100%) relative humidities. *Atmos. Chem. Phys.* 10(3):1329-1344.
32. Prisle NL, Dal Maso M, & Kokkola H (2011) A simple representation of surface active organic aerosol in cloud droplet formation. *Atmos. Chem. Phys.* 11(9):4073-4083.
33. Asa-Awuku A, Nenes A, Gao S, Flagan RC, & Seinfeld JH (2010) Water-soluble SOA from alkene ozonolysis: composition and droplet activation kinetics inferences from analysis of CCN activity. *Atmos. Chem. Phys.* 10(4):1585-1597.
34. Betterton EA & Hoffmann MR (1988) Henry's law constants of some environmentally important aldehydes. *Environ. Sci. Technol.* 22(12):1415-1418.
35. Jayne JT, *et al.* (1992) Uptake of gas-phase aldehydes by water surfaces. *J. Phys. Chem.* 96(13):5452-5460.
36. Romakkaniemi S, *et al.* (2011) Partitioning of semivolatile surface-active compounds between bulk, surface and gas phase. *Geophys. Res. Lett.* 38(3):L03807.
37. Djikaev YS & Tabazadeh A (2003) Effect of adsorption on the uptake of organic trace gas by cloud droplets. *J. Geophys. Res.* 108(D22):4689.
38. Krizner HE, De Haan DO, & Kua J (2009) Thermodynamics and kinetics of methylglyoxal dimer formation: A computational study. *J. Phys. Chem. A* 113(25):6994-7001.
39. Feingold G & Chuang PY (2002) Analysis of the influence of film-forming compounds on droplet growth: Implications for cloud microphysical processes and climate. *J. Atmos. Sci.* 59(12):2006-2018.
40. Conant WC, *et al.* (2004) Aerosol-cloud drop concentration closure in warm cumulus. *J. Geophys. Res.* 109(D13):D13204.
41. Fountoukis C, *et al.* (2007) Aerosol-cloud drop concentration closure for clouds sampled during the International Consortium for Atmospheric Research on Transport and Transformation 2004 campaign. *J. Geophys. Res.* 112(D10):D10S30.
42. Meskhidze N, Nenes A, Conant WC, & Seinfeld JH (2005) Evaluation of a new cloud droplet activation parameterization with in situ data from CRYSTAL-FACE and CSTRIPE. *J. Geophys. Res.* 110(D16):D16202.
43. Moore RH, *et al.* (2012) CCN Spectra, hygroscopicity, and droplet activation kinetics of secondary organic aerosol resulting from the 2010 Deepwater Horizon Oil Spill. *Environ. Sci. Technol.* 46(6):3093-3100.
44. Raatikainen T, Moore RH, Lathem TL, & Nenes A (2012) A coupled observation - modeling approach for studying activation kinetics from measurements of CCN activity. *Atmos. Chem. Phys.* 12(9):4227-4243.
45. Bougiatioti A, *et al.* (2009) Cloud condensation nuclei measurements in the marine boundary layer of the Eastern Mediterranean: CCN closure and droplet growth kinetics. *Atmos. Chem. Phys.* 9(18):7053-7066.
46. Bougiatioti A, *et al.* (2011) Size-resolved CCN distributions and activation kinetics of aged continental and marine aerosol. *Atmos. Chem. Phys.* 11(16):8791-8808.
47. Cerully KM, *et al.* (2011) Aerosol hygroscopicity and CCN activation kinetics in a boreal forest environment during the 2007 EUCAARI campaign. *Atmos. Chem. Phys.* 11(23):12369-12386.
48. Lance S, *et al.* (2009) Cloud condensation nuclei activity, closure, and droplet growth kinetics of Houston aerosol during the Gulf of Mexico Atmospheric Composition and Climate Study (GoMACCS). *J. Geophys. Res.* 114:D00F15.
49. Padró LT, *et al.* (2010) Investigation of cloud condensation nuclei properties and droplet growth kinetics of the water-soluble aerosol fraction in Mexico City. *J. Geophys. Res.* 115(D9):D09204.
50. Tang IN & Munkelwitz HR (1994) Water activities, densities, and refractive indices of aqueous sulfates and sodium nitrate droplets of atmospheric importance. *J. Geophys. Res.* 99(D9):18801-18808.
51. Ruehl CR, *et al.* (2012) Strong evidence of surface tension reduction in microscopic aqueous droplets. *Geophys. Res. Lett.*
52. Kulmala M, *et al.* (1993) The effect of atmospheric nitric acid vapor on cloud condensation nucleus activation. *J. Geophys. Res.* 98(D12):22949-22958.
53. Moore RH, Nenes A, & Medina J (2010) Scanning Mobility CCN Analysis - A method for fast measurements of size-resolved CCN distributions and activation kinetics. *Aerosol Sci. Technol.* 44(10):861-871.
54. Asa-Awuku A, Engelhart GJ, Lee BH, Pandis SN, & Nenes A (2009) Relating CCN activity, volatility, and droplet growth kinetics of β-caryophyllene secondary organic aerosol. *Atmos. Chem. Phys.* 9 (3):795-812.

SUPPORTING INFORMATION

Gas-phase surfactants enhance aerosol cloud nucleation

N. Sareen,[1,†] A. N. Schwier,[1] T. Lathem,[2] A. Nenes, [2,3,*] and V. F. McNeill[1,*]

1. Department of Chemical Engineering, Columbia University, New York, NY 10027
2. School of Earth and Atmospheric Sciences, Georgia Institute of Technology, Atlanta, GA 30332
3. School of Chemical and Biomolecular Engineering, Georgia Institute of Technology, Atlanta, GA 30332
†: Present address: Department of Environmental Sciences, Rutgers University, New Brunswick, NJ 08901
* email: vfm2103@columbia.edu, athanasios.nenes@gatech.edu

Cloud droplet number (CDN) calculations

Computation of droplet number, N_c, is carried out with the Fountoukis and Nenes (FN; 2005) (1) droplet activation parameterization (augmented to account for depletion effects from Giant CCN; Barahona et al., 2010) (2). FN is a comprehensive and efficient formulation, which has been evaluated extensively with numerical simulations (1-3), as well as in situ measurements (4, 5). FN is based on the framework of an ascending adiabatic cloud parcel; N_c is determined by the maximum supersaturation, s_{max}, which is controlled by the water vapor balance and is obtained by classifying the droplets by proximity to their critical diameter ("population splitting"). The effective water vapor uptake coefficient (which affects the water vapor mass transfer coefficient during droplet formation) is set to 0.06, following Fountoukis et al. (2007). (4) The model was integrated for 2 years with present-day emissions of sulfur and sea salt; monthly, grid-by-grid CCN spectra are then derived from the simulations of the second year.

Kinetics of Methylglyoxal Hydration and Oligomerization

Methylglyoxal (MG) rapidly reacts with water in aqueous aerosols to form hydrated methylglyoxal (HMG) according to:

$$MG + H_2O \leftrightarrow HMG \qquad (S1)$$

According to the density functional theory calculations of Krizner et al. (6), the corrected free energy barrier for this process is 17.3 kcal mol^{-1}, and the preexponential factor is 5×10^{11} $M^{-1}s^{-1}$, yielding a pseudo-first-order rate constant at 298 K of approximately 6 s^{-1}. Hence, the time required for methylglyoxal to be 98% converted to its singly hydrated form (7) is ~0.7 s. The apparent enhancement in MG uptake due to hydration is already accounted for in the effective Henry's law constant reported by Betterton and Hoffmann ($H^*=3.2\times10^4$ M atm^{-1}) (7).

The kinetics of methylglyoxal oligomerization in aqueous solutions containing NH_4^+ and H_3O^+ were presented by Sareen et al. (8) It was found that the rate limiting step for the formation of oligomers was the protonation of singly hydrated MG by either NH_4^+ or H_3O^+, with second-order rate constants $k^{II}_{H3O+} \leq 10^{-3}$ $M^{-1}min^{-1}$ and $k^{II}_{NH4+}=5\times10^{-6}$ $M^{-1}min^{-1}$. The conversion rate of HMG, is described by the following equation:

$$R = (k^{II}_{H3O+}[H_3O^+] + k^{II}_{NH4+}[NH_4^+])[HMG] \qquad (S2)$$

In the aerosol experiments presented here, $[NH_4^+]$=28 M and $[H_3O^+]$=7 M. Because the oligomerization reactions are relatively slow compared to the diffusional timescale in the aerosol particle, $\tau=R^2/D$, where R is the characteristic length scale and D is the diffusion coefficient, we expect that the concentration of HMG in the particle is spatially uniform and maintained relatively constant via MG absorption from the gas phase according to Henry's Law. Based on a gas-phase MG concentration of 250 ppb, $[HMG]=8\times10^{-3}$ M. After 3 hours of reaction, the total amount of MG sequestered as oligomeric products is between 2.02×10^{-4} M and 1.03×10^{-2} M. The total concentration of MG and products is then 0.031-6.06x10^{-4} mol C kg^{-1} H_2O.

Inorganic:Organic ratio

This ratio for the chamber filter extracts was calculated based on WSOC and IC analysis. The inorganic on the filter was 1.57x10^4 µg and the water soluble organic matter was 18.928 µg, giving a ratio of 829.4.

For comparison, this ratio is also calculated for the particles in the chamber. Based on 250 ppb of methylglyoxal in the chamber and a Henry's Law constant of 3.2×10^4 M atm^{-1}, the in-particle concentration of methylglyoxal is 0.008 M. Following Tang and Munkelwitz (9), a 0.2 M ammonium sulfate atomizer solution will lead to an in-particle concentration of 14 M at 65 % relative humidity. The inorganic:organic ratio for the chamber based on these numbers is 3209. The ratio of inorganic:organic material in the filter extracts is lower than that predicted based on Henry's Law uptake of methylglyoxal to the particles. This could be due to continued reactive uptake of the gas-phase organic on the filter during particle collection.

Köhler theory analysis (KTA)

The following equations from Moore et al. (10) were used to infer surface tension of the particles:

$$\sigma = \left[\frac{\left(\frac{\rho_o}{M_o}\right)\varepsilon_o \upsilon_o + \frac{\rho_i}{M_i}\varepsilon_i \upsilon_i}{\frac{256}{27}\left(\frac{M_w}{\rho_w}\right)^2 \left(\frac{1}{RT}\right)^3 \omega^{-2}} \right]^{1/3} \quad \text{(S3)}$$

where the subscripts *i*, *o*, and *w* refer to the inorganic, organic, and water respectively. M is the average molecular weight, ρ is the density, ν is the effective van't Hoff factor, R is the universal gas constant, T is the median temperature of the CFSTGC column, σ is the surface tension, and ε is the mass fraction calculated as:

$$\varepsilon_i = \frac{\frac{m_i}{\rho_i}}{\frac{m_i}{\rho_i} + \frac{m_o}{\rho_o}} \quad \text{(S4)}$$

ω, the fitted CCN activity factor, is determined from the critical supersaturation (S_c) and the critical dry activation diameter (d_d) using the equation:

$$S_c = \omega d_d^{-3/2} \quad \text{(S5)}$$

Surface tension of the particle based on Henry's Law

The surface tension of the aerosol particles can be estimated using the Szyszkowski-Langmuir equation:

$$\sigma = \sigma_0 - a\mathrm{T} \ln (1 + b\mathrm{C}) \qquad \text{(S6)}$$

where σ and σ_0 are the surface tension with and without the organics, respectively, T is temperature, C is the carbon content, and *a* and *b* are fit parameters. Although the particles studied here were composed of ammonium sulfate, we are interested in calculating the surface tension of the particle at the moment of activation. At that point, the particle is composed mostly of water. Therefore, values for *a* and *b* are taken from the surface tension measurements done on a methylglyoxal and water solution using pendant drop tensiometry: *a*=0.0244 dyn cm^{-1} K^{-1} and *b*=3.050 kg water (mol C)$^{-1}$. σ_0 was tested in our laboratory using Millipore water and found to be 72.55 dyn cm^{-1}.

C is calculated based on the assumption that the droplet is in Henry's Law equilibrium with the gas phase, and that the total contribution of oligomeric products formed prior to activation is small. Hence based on 250 ppb of methylglyoxal in the chamber (and CFSTGC), we calculate an 8×10^{-3} M methylglyoxal concentration, or 0.0240 mol C (kg water)$^{-1}$. Plugging these values into the Szyszkowski-Langmuir equation gives a value of 72.02 dyn cm^{-1} for the surface tension of the methylglyoxal and ammonium sulfate particles. Surface tension depression will lower the value of κ by a factor of

$$\left(1 - \frac{\Delta\sigma}{\sigma_w}\right)^{-3} \qquad \text{(S7)}$$

where Δσ is the surface tension depression from that of pure water. In our case, the calculated surface tension value of 72.02 dyn cm^{-1} will lead to a very small (2.2%) increase in κ, much less than the enhancement in CCN activity seen in our chamber studies.

For acetaldehyde, the constants *a* and *b* are taken from the surface tension measurements done on an acetaldehyde and water solution using pendant drop tensiometry: *a*=0.0037 dyn cm^{-1} K^{-1} and *b*=491.64 kg water (mol C)$^{-1}$ (11). Based on 250 ppb of acetaldehyde in the chamber and a Henry's Law constant of 11.4 M/atm, the acetaldehyde concentration in a particle is 2.85 x 10^{-6} M, or 5.7 x 10-^{6} mol C (kg water)$^{-1}$. These values give a surface tension of 73.16 dyn cm^{-1} for the surface tension of the acetaldehyde and ammonium sulfate particles and will lead to a negligible change in κ of 0.01%.

Concentration of methylglyoxal at the moment of activation

The critical wet diameter, D_c, is

$$D_c = \left(\frac{3\kappa}{A}\right)^{0.5} d_d^{1.5} \qquad \text{(S8)}$$

where, κ is the hygroscopicity parameter, calculated from CCN activity data following Petters and Kreidenweis (12), and

$$A = \frac{4\,\sigma M_w}{RT\rho_w} \qquad \text{(S9)}$$

Based on the amount of methylglyoxal in the chamber, 250 ppb, we can calculate the number of molecules of methylglyoxal at each d_d. Since the number of molecules is constant in the particle, it can be divided by the corresponding volume at D_c to get the concentration at the activated diameter.

In the chamber experiments, the estimated concentration of methylglyoxal in the particles at the moment of activation (using Henry's Law) ranged from 1.17x10^{-5} – 3.22x10^{-5} M and for the filter extracts it was 1.24x10^{-4} – 4.53x10^{-5} M, orders of magnitude lower than for the atomized bulk solutions (1.59x10^{-2} – 2.86x10^{-3} M).

Calibration of supersaturation in the CCN counter

The effective supersaturation in the CCN instrument depends on the flow rate, pressure and temperature gradient applied on the column (13). Scanning Mobility CCN Analysis (SMCA) with $(NH_4)_2SO_4$ calibration aerosol is used to determine supersaturation for a given set of operating conditions, following the procedure of Moore et al. (2010) (10). Calibration aerosol is generated by atomizing an ammonium sulfate solution in pure water. Atomized droplets were dried in a silica gel dryer and sampled by a differential mobility analyzer (DMA; TSI 3081 Long DMA) that classifies the aerosol and then introduced into the CFSTGC and a Condensation Particle Counter (CPC; TSI 3010). The voltage applied to the DMA was scanned, and inversion of the time series of CCN and CPC counts yields the fraction of classified particles that act as CCN ("activation curve"). The dry mobility diameter for which half of the classified particles act as CCN, d_{50}, is used to characterize instrument supersaturation (being equal to the critical supersaturation of particles with dry diameter equal to d_{50}). Köhler theory is used to compute the effective instrument supersaturation, assuming the $(NH_4)_2SO_4$ particles have (at the point of activation) the surface tension and density of pure water, and a variable van't Hoff factor is used as described in Moore et al. (2010) (10).

The use of non-acidified $(NH_4)_2SO_4$ as the control

We have used ISORROPIA to compare the apparent hygroscopicity parameter, κ, for the acidified and non-acidified $(NH_4)_2SO_4$. The $(NH_4)_2SO_4$ compositions at pH = 0 and 2 are determined as follows: pure 0.2 M $(NH_4)_2SO_4$ is taken and enough H_2SO_4 is added so that the pH is 0 and 2, respectively. Assuming that H_2SO_4 (SA) and NH_4HSO_4 (AB) dissociate completely in solution, we have that the dry material is 37% (by mass) AB + 63% SA for the pH 0 aerosol, and, 6% AB + 94% $(NH_4)_2SO_4$ for the pH=2 aerosol.

These compositions are then used in ISORROPIA to determine the amount of water associated with each constituent (SA, AB, $(NH_4)_2SO_4$) at various RH values. Given that our dryer reaches 5-10% RH, for the pH=

0 solution there is about 25% (by volume) water. This is justified as H_2SO_4 is so hygroscopic, that it never releases all of its water even at single-digit RH. The particle sized at 5-10% RH will have 75% volume of salt and the rest is water. κ is then calculated to be ~0.6. Similar results are seen for the pH=2 aerosol.

In both the acidified cases, κ is predicted to be close to that of pure $(NH_4)_2SO_4$, and hence we can use pure $(NH_4)_2SO_4$ as the control in our studies.

Depletion of methylglyoxal in the gas phase

We operate our chamber as a continuous flow stirred tank reactor. That is, after the initial startup period, conditions are at steady-state inside the chamber, and the residence time for gases and particles in the chamber, τ, is given by

$$\tau = \frac{V}{F}$$

where V is the reactor volume (3.5 m^3) and F is the total volumetric flowrate through the reactor.

We calculate the depletion of methylglyoxal in the chamber in two ways, firstly, assuming that Henry's Law uptake is valid and secondly, based on surface adsorption.

Henry's Law Uptake. Assuming Henry's Law describes the uptake of gas-phase methylglyoxal (MG) to the particles, the particle-phase concentration of MG is directly proportional to the gas-phase concentration according to:

$$[MG]_{aq} = H^* P_{MG}$$

where H^* is the effective Henry's Law constant. From Betterton and Hoffman (1988), $H^* = 3.2\times10^4$ M atm^{-1}. Hence, with 250 ppb MG in the gas phase, $[MG]_{aq} = 8\times10^{-3}$ M.

After the particles have equilibrated with MG in the chamber, the maximum amount of MG taken up from the gas phase will be:

$$\text{uptake} = N_p V_p [\text{MG}]_{aq} N_A = 2.5 \times 10^{11} \text{molec}/(\text{cm}^3 \text{ gas})$$

here, $N_p \approx 10^6$ particles/(cm^{-3} gas), $V_p = \frac{4}{3}\pi(231 \times 10^{-7} \text{ cm})^3 \left(\frac{1\,L}{1000 \text{ cm}^3}\right)$ [=] L particle^{-1}, and N_A = Avogadro's number. 250 ppb corresponds to a total initial gas-phase MG concentration of 6.15×10^{12} molec cm^{-3}. Therefore, uptake of MG to the particles will deplete the gas-phase concentration by at most 4%. For the 8 ppb MG case, the depletion is negligible.

Surface Adsorption. We may also assume a model of adsorption of gas-phase MG to the particle surface. A reasonable estimate is that each MG molecule occupies 50 Å^2 on the surface. In this case, the formation of a full monolayer of MG on one 203 nm (surface-weighted) particle will result in the uptake of 1.04×10^6 molecules of MG. There are no experimental data available to allow us to predict the surface coverage as a function of MG partial pressure so we will assume full monolayer coverage in these calculations.

After the particles have equilibrated with MG in the chamber, the maximum amount of MG taken up from the gas phase (per cm^3 of gas) will be 1.04×10^{12} molec cm^{-3} of MG, 5x that taken up in the Henry's Law scenario. This would result in up to 16% depletion of gas-phase MG. For the 8 ppb MG, we estimate 14% depletion.

We also performed similar calculations for observed concentrations in the atmosphere (urban: 10^4 cm^{-3}, 2.5 ppb MG; wet-season Amazon: 10^2 cm^{-3}, 0.125 ppb MG). Based on Henry's Law, we calculate negligible depletion for both urban and wet-season Amazon. Taking into account only surface adsorption, we calculate 17% depletion in the urban scenario and 3% depletion in the Amazon. Hence we do not anticipate depletion effects to be prominent. Given that we are considering full monolayer

coverage, these calculations represent the upper limit for depletion. For acetaldehyde, we expect lesser depletion since its Henry's Law constant is 1000 times smaller than methylglyoxal and it is also slightly more prominent in the atmosphere as compared to methylglyoxal.

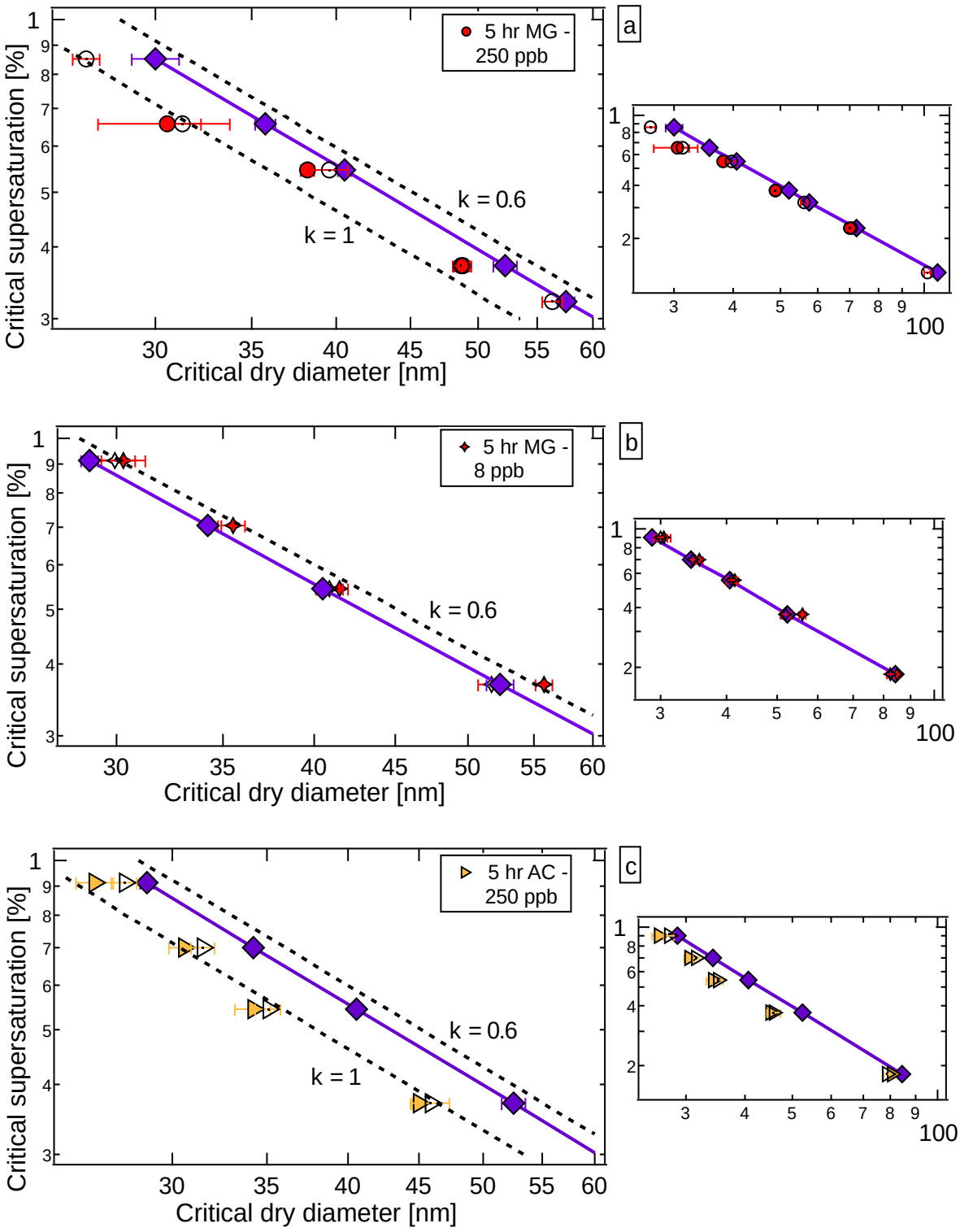
a
5 hr MG - 250 ppb
k = 0.6
k = 1
Critical supersaturation [%]
Critical dry diameter [nm]
b
5 hr MG - 8 ppb
k = 0.6
Critical supersaturation [%]
Critical dry diameter [nm]
c
5 hr AC - 250 ppb
k = 0.6
k = 1
Critical supersaturation [%]
Critical dry diameter [nm]

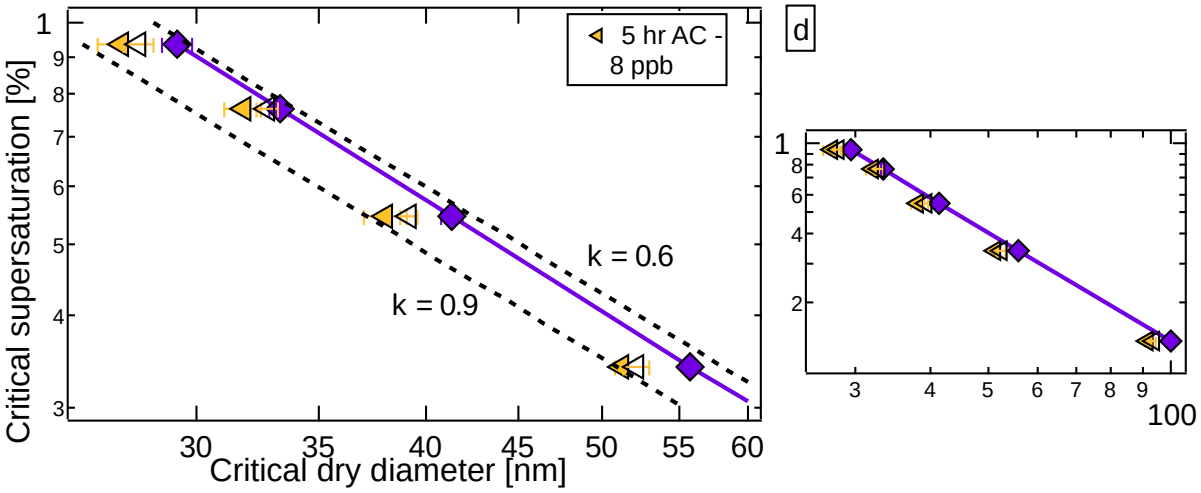
5 hr AC - 8 ppb
k = 0.6
k = 0.9
Critical supersaturation [%]
Critical dry diameter [nm]
d

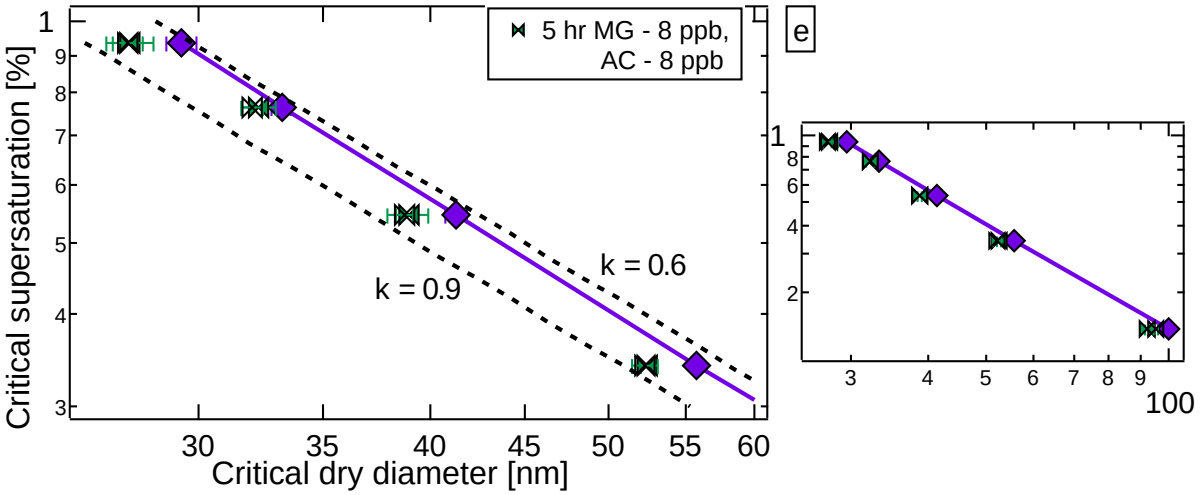
5 hr MG - 8 ppb, AC - 8 ppb
k = 0.6
k = 0.9
Critical supersaturation [%]
Critical dry diameter [nm]
e

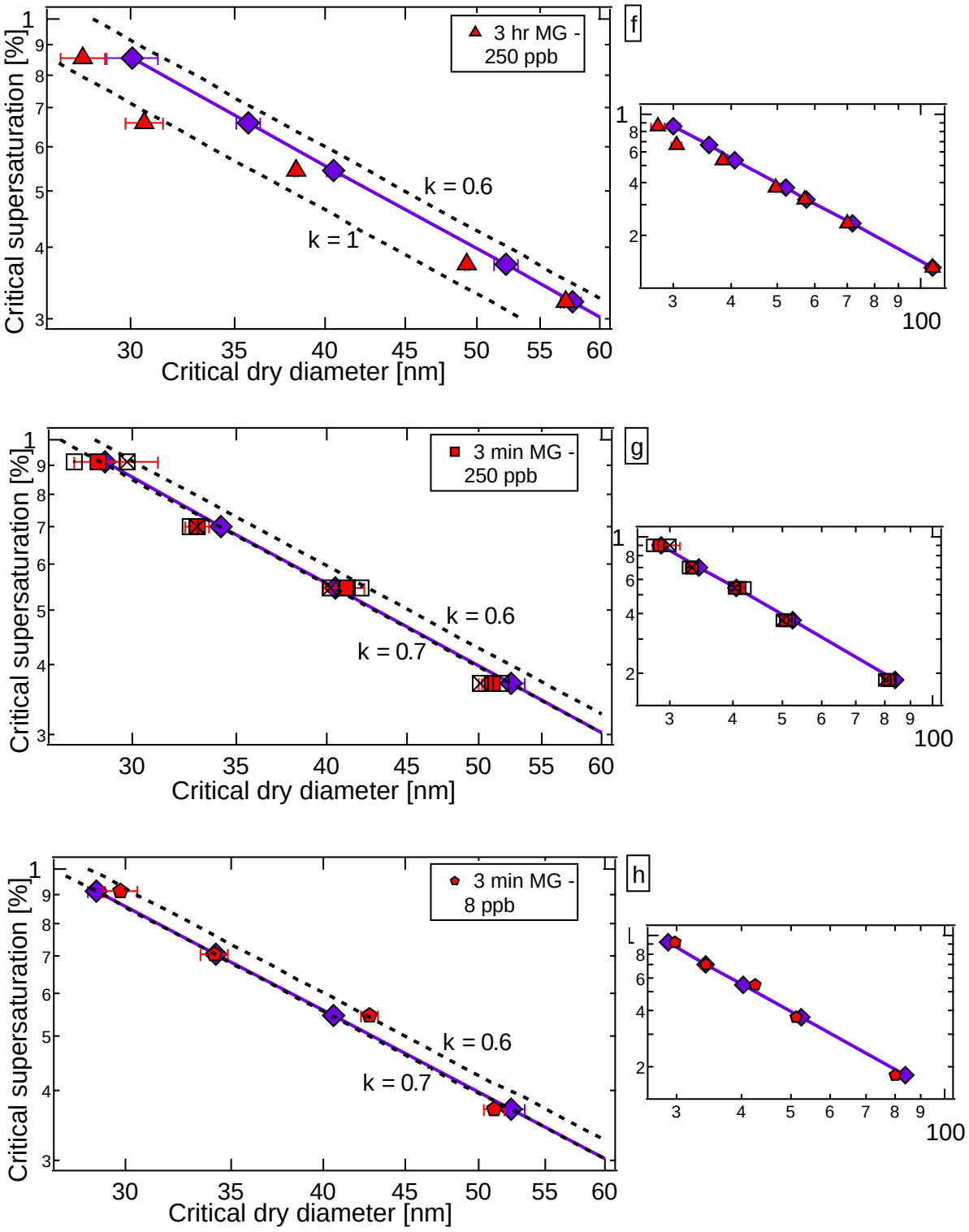

Supplementary Figure S1: Cloud condensation nuclei (CCN) activity data. Humidified, acidifed $(NH_4)_2SO_4$ aerosols were exposed to gas-phase methylglyoxal or acetaldehyde in a 3.5 m^3 Teflon reaction chamber or a glass flow tube for varying residence times. The critical dry diameters observed for each experiment as a function of instrument supersaturation are compared to the

$(NH_4)_2SO_4$ control (purple diamonds) in order to demonstrate the effect of organics. Closed and open symbols represent the first and second trials for each time point, respectively. The small graphs on the right side represent the entire range of supersaturations studied, whereas the main plots zoom in on the smaller diameters. The dashed lines show values of constant κ, ranging from our $(NH_4)_2SO_4$ control (κ~0.6) to the maximum κ value observed for each experiment. Panels (a) and (b) show the results for particles exposed to 250 ppb and 8 ppb of methylglyoxal for 5 h, respectively. Panels (c) and (d) show the results for particles exposed to 250 ppb and 8 ppb of acetaldehyde for 5 h, respectively. In panel (e), particles were exposed to 8 ppb of methylglyoxal and 8 ppb of acetaldehyde for 5 h. In panel (f), particles were exposed to 250 ppb of methylglyoxal for 3 h. Panels (g) and (h) show the results for particles exposed to 250 ppb and 8 ppb of methylglyoxal for 3 min in the flowtube reactor, respectively.

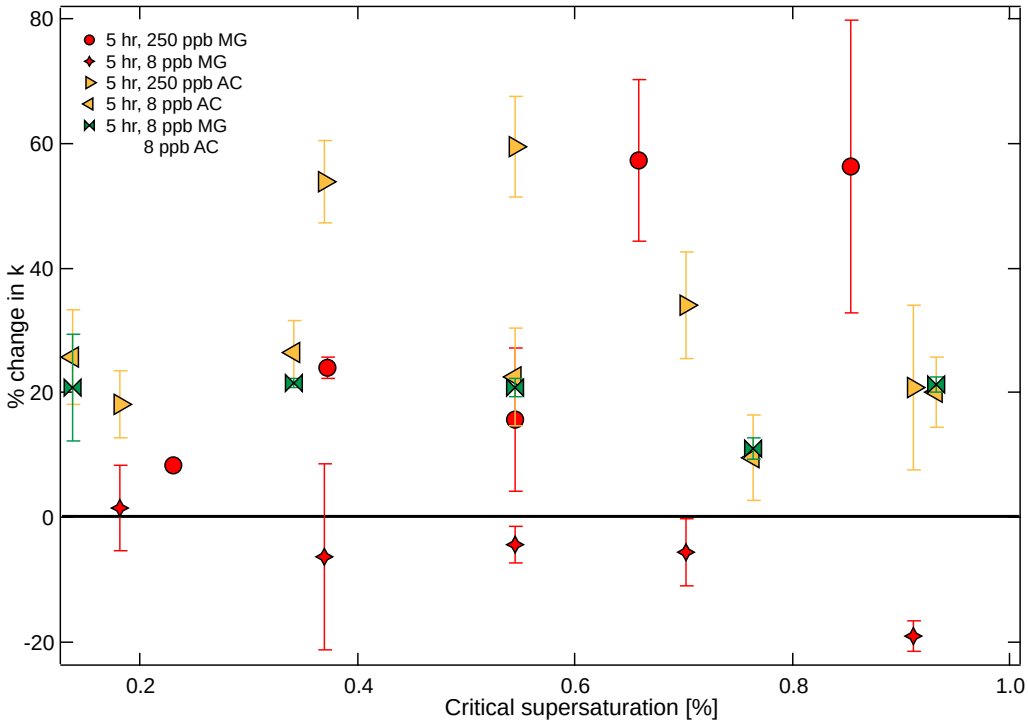

Supplementary Figure S2: Hygroscopicity parameter, κ, data. Humidified, acidified $(NH_4)_2SO_4$ aerosols were exposed to gas-phase methylglyoxal or acetaldehyde in a 3.5 m^3 Teflon reaction chamber. The κ values for each experiment as a function of instrument supersaturation are compared to the $(NH_4)_2SO_4$ control in order to demonstrate the effect of organics. The data shown here are the results for $(NH_4)_2SO_4$ particles exposed to 250 ppb and 8 ppb of methylglyoxal for 5 h, particles exposed to 250 ppb and 8 ppb of acetaldehyde for 5 h, and finally particles exposed to a mixture of 8 ppb of methylglyoxal and 8 ppb of acetaldehyde for 5 h.

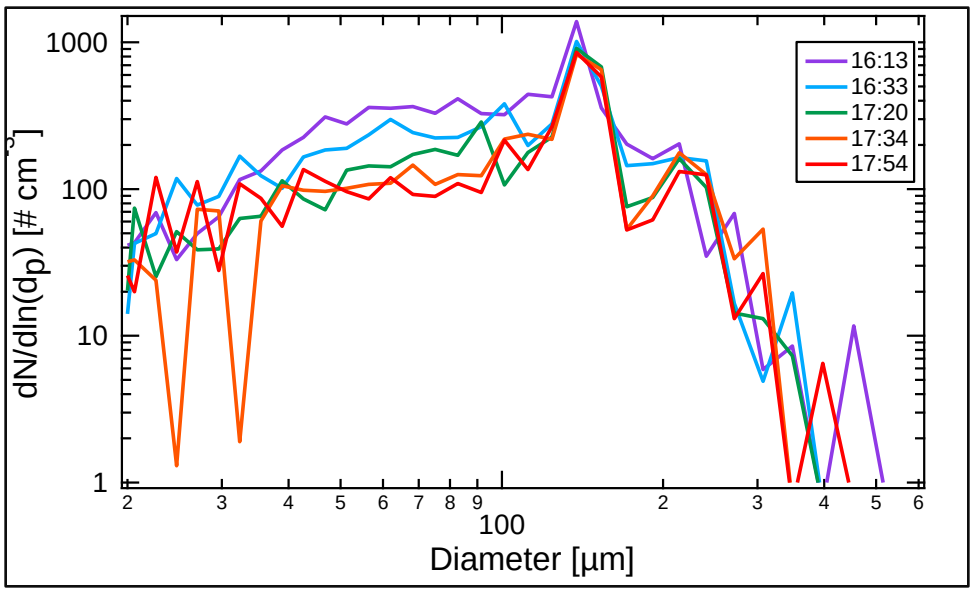

Supplementary Figure S3: SMPS data showing the number size distribution of particles over time. 150 nm particles were size-selected using the DMA and put into the chamber. As can be seen, there is negligible particle growth.

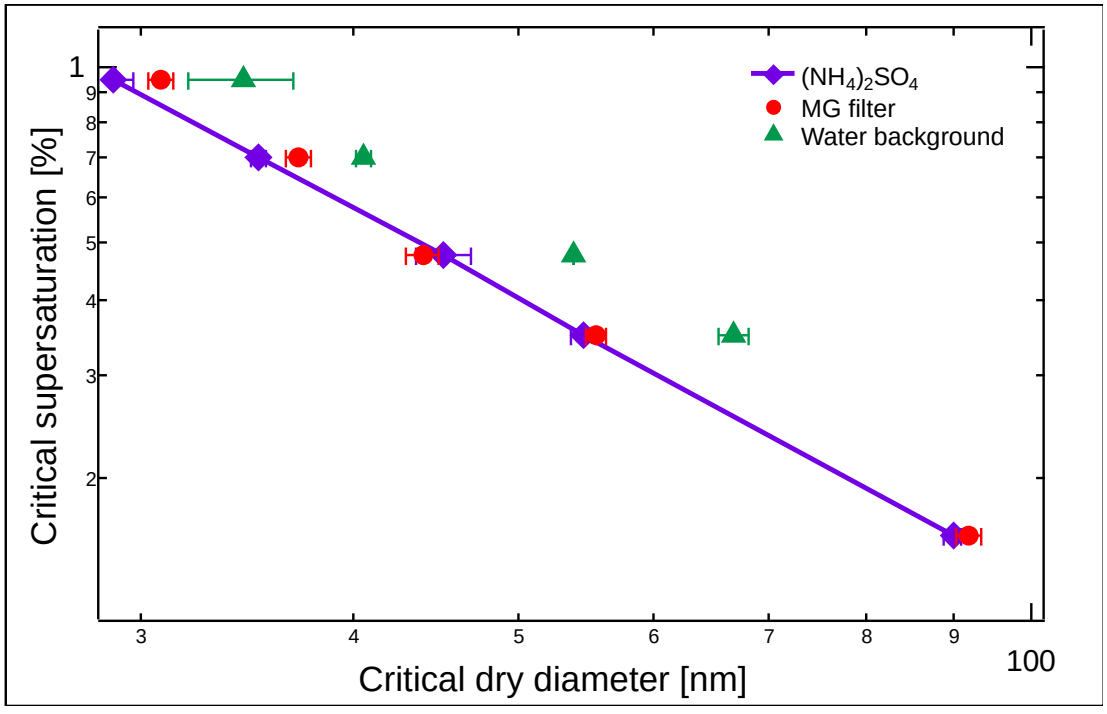

Supplementary Figure S4: CFSTGC data of the extracted filter samples obtained by pumping down the chamber for ~14 h following the 5 h run. The dry diameters are compared to the $(NH_4)_2SO_4$ control.

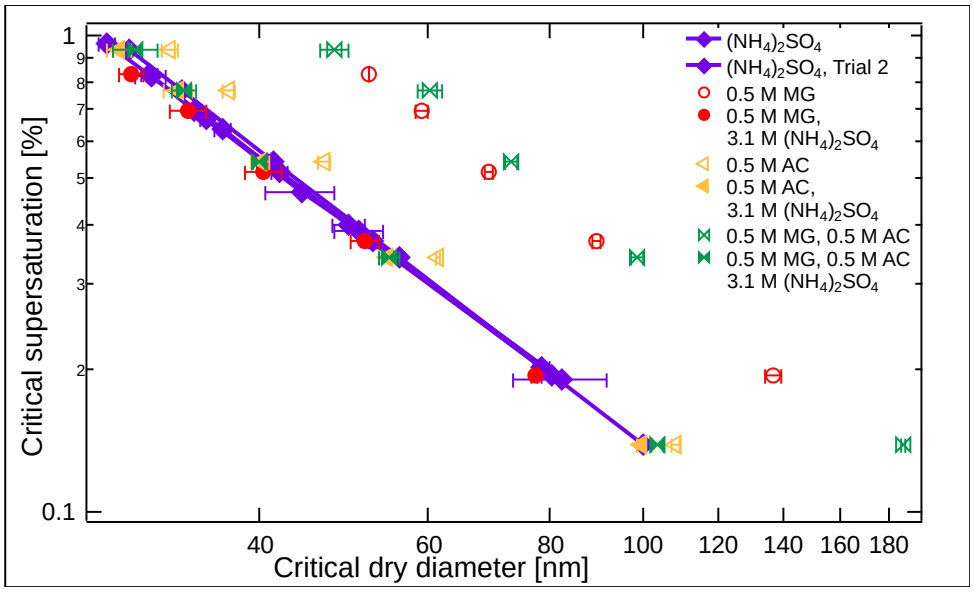

Supplementary Figure S5: CFSTGC data from organics in solution compared to the $(NH_4)_2SO_4$ control. The plot includes: $(NH_4)_2SO_4$ solution, methylglyoxal solution, methylglyoxal/$(NH_4)_2SO_4$ solution, acetaldehyde solution, acetaldehyde/$(NH_4)_2SO_4$ solution, methylglyoxal/acetaldehyde solution, and methylglyoxal/acetaldehyde/$(NH_4)_2SO_4$ solution.

Supplementary Table S1: Exponents of the power log fits for the SS vs dry diameter graphs for the various chamber experiments. As expected, these values deviate from the pure AS calibration curve.

Experiment	Average power log fits (exponent)
$(NH_4)_2SO_4$	-1.52±0.03
5 hr 250 ppb MG	-1.34±0.09
3 hr 250 ppb MG	-1.37
3 min 250 ppb MG	-1.42±0.03
5 hr 8 ppb MG	-1.34±0.09
3 min 8 ppb MG	-1.51
5 hr 250 ppb AC	-1.47±0.06
5 hr 8 ppb AC	-1.59±0.001
5 hr 8 ppb AC, 8 ppb MG	-1.57±0.04

Supplementary Table S2: Hygroscopicity parameter, κ, values for the different bulk studies. Bulk aqueous solutions containing 0.5 M of the organic (methylglyoxal and/or acetaldehyde) with and without 3.1 M $(NH_4)_2SO_4$ were allowed to react for 24 h, and were then atomized and analyzed using the CFSTGC.

Experiment	Average κ
$(NH_4)_2SO_4$	0.60±0.18
0.5 M MG	0.12±0.04
0.5 M MG, 3.1 M $(NH_4)_2SO_4$	0.68±0.09
0.5 M AC	0.44±0.13
0.5 M AC, 3.1 M $(NH_4)_2SO_4$	0.62±0.19
0.5 M MG, 0.5 M AC	0.11±0.03
0.5 M MG, 0.5 M AC, 3.1 M $(NH_4)_2SO_4$	0.59±0.18

Supplementary Table S3: Statistical analysis for hygroscopicity parameter, κ. T-test at the 90% confidence level is conducted for the various chamber experiments, to determine how statistically different they are from the $(NH_4)_2SO_4$ control.

Experiment	t	p
5 hr 250 ppb MG	-3.36	0.0153
5 hr 8 ppb MG	2.072	0.107
5 hr 250 ppb AC	-4.24	0.0133
5 hr 8 ppb AC	-5.82	0.0043
5 hr 8 ppb AC, 8 ppb MG	-8.18	0.0012

References

1. Fountoukis C & Nenes A (2005) Continued development of a cloud droplet formation parameterization for global climate models. *J. Geophys. Res.* 110(D11):D11212.
2. Barahona D*, et al.* (2010) Comprehensively accounting for the effect of giant CCN in cloud activation parameterizations. *Atmos. Chem. Phys.* 10(5):2467-2473.
3. Ghan S (2011) Droplet Nucleation: Physically-Based Parameterizations and Comparative Evaluation. *Journal of Advances in Modeling Earth Systems* 3(M10001):33 pp.
4. Fountoukis C*, et al.* (2007) Aerosol-cloud drop concentration closure for clouds sampled during the International Consortium for Atmospheric Research on Transport and Transformation 2004 campaign. *J. Geophys. Res.* 112(D10):D10S30.
5. Meskhidze N, Nenes A, Conant WC, & Seinfeld JH (2005) Evaluation of a new cloud droplet activation parameterization with in situ data from CRYSTAL-FACE and CSTRIPE. *J. Geophys. Res.* 110(D16):D16202.
6. Krizner HE, De Haan DO, & Kua J (2009) Thermodynamics and kinetics of methylglyoxal dimer formation: A computational study. *The Journal of Physical Chemistry A* 113(25):6994-7001.
7. Betterton EA & Hoffmann MR (1988) Henry's law constants of some environmentally important aldehydes. *Environmental Science & Technology* 22(12):1415-1418.
8. Sareen N, Schwier AN, Shapiro EL, Mitroo D, & McNeill VF (2010) Secondary organic material formed by methylglyoxal in aqueous aerosol mimics. *Atmos.Chem.Phys.* 10 (3):997-1016.
9. Tang IN & Munkelwitz HR (1994) Water activities, densities, and refractive indices of aqueous sulfates and sodium nitrate droplets of atmospheric importance. *J.Geophys.Res.* 99(D9):18801-18808.
10. Moore RH, Nenes A, & Medina J (2010) Scanning Mobility CCN Analysis - A method for fast measurements of size-resolved CCN distributions and activation kinetics. *Aerosol Science and Technology* 44(10):861-871.
11. Li Z, Schwier AN, Sareen N, & McNeill VF (2011) Reactive processing of formaldehyde and acetaldehyde in aqueous aerosol mimics: Surface tension depression and secondary organic products. *Atmos. Chem. Phys.* 11(22):11617-11629.
12. Petters MD & Kreidenweis SM (2007) A single parameter representation of hygroscopic growth and cloud condensation nucleus activity. *Atmos.Chem.Phys.* 7(8):1961-1971.
13. Lance S, Medina J, Smith JN, & Nenes A (2006) Mapping the Operation of the DMT Continuous Flow CCN Counter. *Aerosol Science and Technology* 40(4):242-254.